properties of the PET-based resins are being investigated and will be reported in a subsequent publication.

PET-based resins would be best suited for processes like hot moulding, where a higher viscosity is desirable. These PET-based resins would definitely benefit the FRP industries by offering versatility in processing and properties over conventional resins.

Registry No. PET, 25038-59-9; PG, 57-55-6; (EG)(PG)-(TPA)(maleic anhydride)(copolymer), 30790-78-4; $C_6H_5CH{=}CH_2$, 100-42-5.

Literature Cited

Boeing, H. V. In *Encyclopedia of Polymer Science and Technology*; Wiley: New York, 1969; Vol. 11, p 150.
Etienne, Y.; Soulas, R. US Patent 869 017, 1969.
Heinge, J.; Kuehnpast, W.; Ramm, H.; Richardt, H. Ger (East) Patent 68 500, 1969.
Hemmi, H.; Nagashima, H.; Kimura, Y.; Teresaki, I.; Satani, M. Jap. Kokai Patent 7 362 732, 1973.
Ligorati, F.; Aglietti, G.; Nova, V. E. Ger. Offen. Patent 2 158 560, 1972.
Makimura, O.; Miyake, H. Jap. Patent, 7 809 275, 1978.
Matsuura, M.; Habara, T.; Katagiri, Y.; Jap. Kokai Patent 7 571 639, 1975.
Miura, K.; Kagiya, Y.; Ichikawa, T. Jap. Patent 6 823 449, 1968.
Miyake, H.; Makimura, O.; Tsuchida, T. Ger. Offen. Patent 2 506 744, 1975.
Modern Plastics International; McGraw Hill: Switzerland, 1986; Vol. 16, No. 1, p 26.
Mueller, W.; Groeger, C.; Schmidt, W.; Strobel, L. Patent Ger (East) 92 801, 1972.
Ostrowski, H. S. US Patent 3 884 850, 1975.
Parkyn, B.; Lamb, F.; Clifton, B. V. *Polyesters*; American Elsevier: New York, 1967; Vol. 2, Chapter 2.
Rustagi, S. C.; Dabholkar, D. P. A.; Niham, J. K.; Marathe, M. N.; Iyer, K. B. Indian Patent 145 323, 1977.
Sittig, M. *Organic and Polymer Waste Reclaiming Encyclopedia*; Noyes Data: Englewood Cliffs, NJ, 1981; pp 41, 117.
Tong, S. N.; Chen, D. S.; Chen, C. C.; Chung, L. Z. *Polymer* **1983**, *24*, 469.
Toshima, H. Jap. Kokai Patent 7 564 382, 1975.
Urbanski, J.; Czerwinski, W.; Janika, K.; Majewska, F.; Zowall, H.; *Handbook of Analysis of Synthetic Polymers and Plastics*; Ellis Horwood: Chichester, England, 1977.

Received for review May 7, 1986
Accepted August 14, 1986

Vapor-Phase Esterification of Acetic Acid with Ethanol Catalyzed by a Macroporous Sulfonated Styrene–Divinylbenzene (20%) Resin

Jaime Giménez,* José Costa, and Salvador Cervera
Department of Chemical Engineering, Faculty of Chemistry, University of Barcelona, 08028 Barcelona, Spain

The kinetics of the vapor-phase (85–120 °C) esterification of acetic acid with ethyl alcohol, at atmospheric pressure, catalyzed by a macroporous sulfonated styrene–divinylbenzene (DVB; 20%) resin, has been studied. A simple first-order model ($r = k'p_1$) fits experimental kinetic data properly for a constant reactants ratio. Discussion by means of L–H–H–W models shows that the rate-controlling step is the surface reaction with a single-site mechanism. The apparent activation energy is 4000 cal/mol.

The esterification reaction of acetic acid with ethanol has been widely studied, mainly because of its industrial interest. Ethyl acetate is a very known solvent with many applications.

This reaction has been studied in the vapor phase using solid catalysts, like silica gel, silica–alumina, aluminum orthophosphate, zeolites, several metal oxides, etc. (Amundson and Stusiak, 1959; Ballesteros et al., 1967; Buckley and Altpeter, 1951; Chashchin, 1963; Hoerig et al., 1943; Santacesaria et al., 1983; Sinisterra et al., 1979; Venkateswarlu et al., 1958). Its kinetics is still a matter of discussion, and the rate-limiting steps are not always clear enough.

There are also a few kinetic studies done with ion-exchange resins as catalysts. In all of them, gel-type sulfonated styrene–divinylbenzene (DVB) resins have been used (Andrianova and Bruns, 1960; Andrianova, 1962, 1964; Herrman, 1955). Kinetic data interpretations are controversial, and modeling is far from being completed.

Research in catalysis by ion-exchange resins is undoubtedly interesting, not only under a pure physicochemical point of view but because of the advantages of these types of catalysts over the conventional ones. Ion-exchange resins increase the product yield, keep their activity a long time, and do not pollute; it is easy to separate them from reaction media and to regenerate them (Costa et al., 1984; Polyanskii and Sapozhnikov, 1977). They also have some disadvantages: they are less resistant to temperature and abrasion and are more expensive. However, accounting for the savings of the advantages mentioned involve, it is not risky to predict an important growth in their industrial catalytic applications.

Concerning the accessibility of the resin-active sites in vapor-phase reactions, the catalytic performance of resins has been improved with the use of the macroporous-type ones.

Acetic acid–ethanol esterification had not been previously studied using macroporous-type resins. This fact and the preceding aspects were the starting point of this work. The aim of this study has been the kinetic study of this esterification reaction with a macroporous-type sulfonated resin, in order to obtain phenomenological rate equations and discuss them according to L–H–H–W models criteria.

Experimental Section

(i) Apparatus. The experimental kinetic work was carried out in a continuous-flow device at atmospheric pressure (see Figure 1).

The two liquid reactants were fed to the vaporizer with either a syringe pump or a Mariotte-type buret, depending on the flow rates used. A good performance of the vaporizer is paramount, given that this esterification reaction is autocatalytic when conducted in the liquid phase, and so condensation has to be avoided. Nitrogen was used as

0888-5885/87/2626-0198$01.50/0

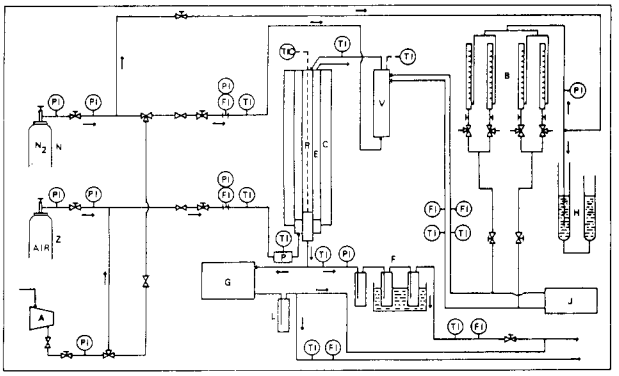

Figure 1. Schematic flow diagram of the apparatus: R, reaction chamber; E, external fluidized sand bed; C, cylindric heating device; V, vaporizer; P, air preheater; B, Mariotte-type burets; H, mercury presostate; J, syringe pump; A, air compressor; G, gas chromatograph; F and L, traps.

an inert gas to drive the vaporized reactants into the reaction chamber, thus controlling gas-phase homogeneity and the reactants' partial pressures.

The reaction chamber was a Pyrex tube (length, 67 cm; internal diameter, 2 cm) with a porous plate to hold the catalyst bed. This chamber was housed concentrically in a jacketed tube which consisted of an external fluidized sand bed to keep the reaction bed isothermal. The ensemble was placed, also concentrically, in a cylindric heating device.

(ii) Chemical Analysis. The analysis of the outgoing gas was continuously performed by a gas chromatograph (HP 5840A) supplied with a gas valve. The elution volume was 0.5 cm^3. A Chromosorb 101 (80/100) column (3 m × $^1/_8$ in.) and helium as the carrier gas were employed.

(iii) Catalyst. Amberlyst-15 (Rohm and Haas) was used as the catalyst. It is a macroporous-type sulfonated styrene–DVB (20%) resin, strongly acid. Catalyst batches of different particle sizes were prepared in our laboratory. Neither trituration nor particle diameter affected the ion-exchange capacity of the resin. It was 4.53 mequiv/g (gram of dry resin).

Results and Discussion

(i) Kinetic Control: Previous Study. The first stage of the work was to choose experimental conditions where the process rate was controlled by chemical steps.

To attain this, the following verifications were done.

(1) There were not any homogeneous reactions.

(2) There were not any appreciable side reactions. Only nonsignificant amounts of ethyl ether were produced in certain experiments.

(3) Chemical equilibrium was not reached for conversions under 85%, according to Hawes' equations (Hawes and Kabel, 1968).

(4) Differential reaction could be assumed up to 25–30% conversions.

(5) Given the very high catalyst activity, an inert solid (quartz) had to be used to have reaction beds with a suitable height/diameter ratio. This ratio did not influence the process rate in the range 0.2–3. Inert/catalyst ratios less than 25 did not affect the process rate either.

(6) External mass transfer was not rate limiting for the tested range of Reynolds numbers that are larger than 0.1.

(7) Internal diffusion was not rate controlling for particle diameters smaller than 0.8 mm.

(8) Acetic acid dimerized in the vapor phase (Potter et al., 1955; Santacesaria et al., 1983). This fact was taken into account in the partial pressure and kinetic calculations.

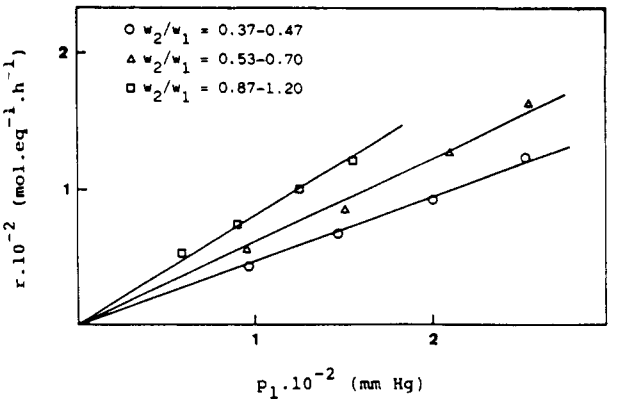

Figure 2. Reaction rate variation vs. ethanol partial pressure for experiments in differential conditions (T = 118 °C).

Table I. Comparison of k' Values Obtained by Differential and Integral Treatments

$(w_2/w_1)_m$	k',[a] mol·equiv^{-1}·h^{-1}·mmHg^{-1}	k',[b] mol·equiv^{-1}·h^{-1}·mmHg^{-1}
0.42	0.447 < 0.47 < 0.499	0.434 < 0.46 < 0.477
0.61	0.571 < 0.62 < 0.662	0.563 < 0.59 < 0.625
1.01	0.747 < 0.80 < 0.861	0.775 < 0.87 < 0.959

[a] $r = k'p_1$. [b] $Y' = k'(Q/w_{1E})$.

(ii) Phenomenological Kinetic Expressions. (a) Partial Pressures Influence. Kinetic experiments were performed at a constant temperature and when varying methodically the reactants partial pressures. Conversions were maintained in the differential reaction range. The results are shown in Figure 2. There is a linear relationship between the reaction rate and the ethanol partial pressure, if the feed reactants ratio is fixed. Thus, the potential expression

$$r = k'p_1 \tag{1}$$

fits these data well. The constant k' is a function of the reactants ratio, and it will be discussed later.

Because of the simplicity of the former expression, an integral treatment is easy to develop. The reactor mass balance, assuming the plug flow hypothesis, is

$$\int_0^{X_1} dX_1/r = Q/w_{1E} \tag{2}$$

If we consider that (1) the reactants ratio does not vary much through the reactor (it should be constant according to the reaction stoichiometry, but acetic acid dimerization affects this ratio a little) and (2) it is possible to define a linear relationship between the pressure drop through the catalyst bed and the reaction conversion

$$P = P_E(1 - fX_1) \tag{3}$$

then the integrated expression is

$$Y' = k'(Q/w_{1E}) \tag{4}$$

where

$$Y' = \frac{1}{x_{1E}P_E(1-f)} \ln\left(\frac{1 - fX_1}{1 - X_1}\right) \tag{5}$$

The kinetic data fit this equation well, as shown in Figure 3.

The k' constant values are given in Table I. The confidence interval limits have been estimated for a significance level of 0.05. Good agreement between differential and integral treatments is observed.

(b) Temperature Effect. Kinetic experiments were performed when the reaction temperature and the reac-

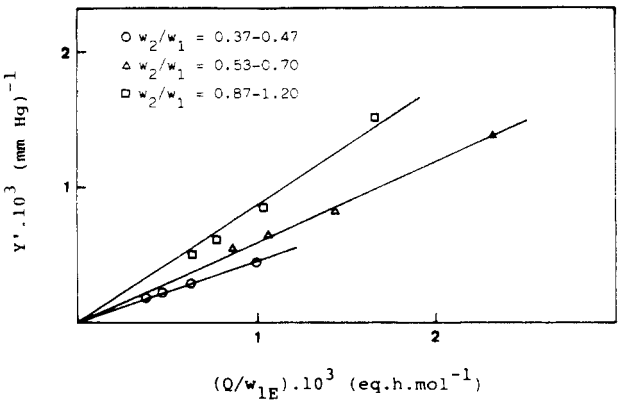

Figure 3. Variation of parameter Y' vs. space time.

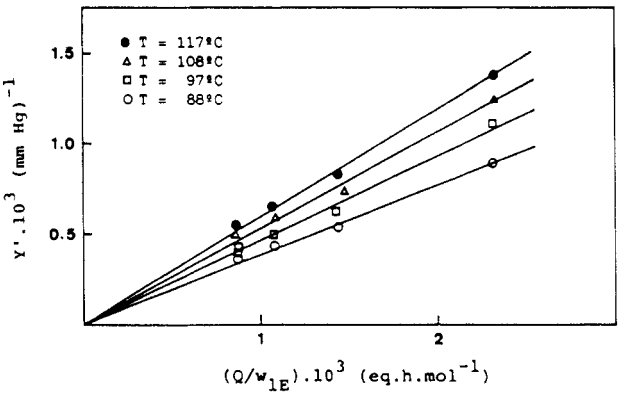

Figure 4. Variation of parameter Y' vs. space time at different temperatures.

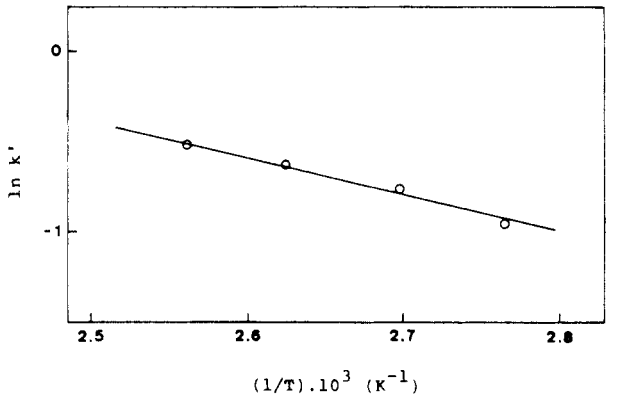

Figure 5. Arrhenius plot according to values shown in Figure 4.

tants partial pressures were varied systematically.

The results are shown in Figure 4. The simple linear expressions 1 and 4 are applicable to the tested temperature interval (85–120 °C).

The k' constant values are correlated with the respective temperature ones, according to the Arrhenius equation (Figure 5). The fitting of the Arrhenius model and the consequent parameter estimation were done by least-squares weighted nonlinear estimation, following the Gauss–Seidel method. The fitted expression is

$$k' = 100e^{-4000/RT} \tag{6}$$

where the activation energy is given in cal/mol and the preexponential factor in mol·equiv^{-1}·h^{-1}·mmHg^{-1}.

Variances, confidence intervals, and confidence regions were estimated, pointing out the goodness of the Arrhenius equation fitting.

(iii) L–H–H–W Models. The simple phenomenological kinetic model obtained can be explained by means of the L–H–H–W models. A classical treatment, that is, taking

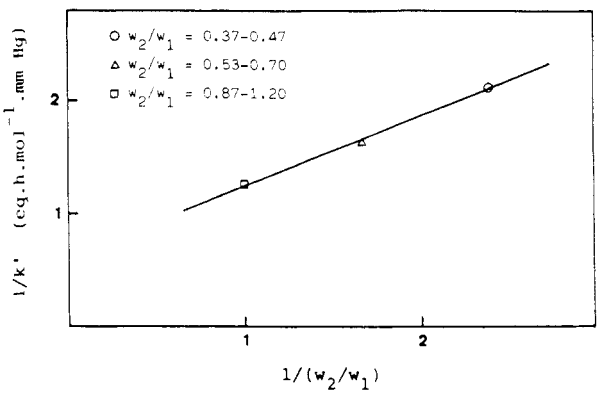

Figure 6. Variation of the reciprocal of k' vs. the reciprocal of the reactants ratio. The values shown correspond to those in Table I for the $r = k'p_1$ model. w_2/w_1 data are the mean values for each of the three experimental series.

Table II. Parameters Corresponding to Single-Site or Dual-Site Mechanisms in L–H–H–W Models

model	k, mol·equiv^{-1}·h^{-1}·mmHg^{-2}	K_1, mmHg^{-1}	K_2, mmHg^{-1}
single-site	0.039	0.024	0.015
dual-site	0.020	0.0034	0.0024

into account the three possible rate-limiting steps, reactants adsorption, surface reaction, and products desorption, and the relevant hypothesis, gives several equations to be checked with the phenomenological kinetic behavior. Only the assumption that the process rate is controlled by a surface reaction step is consistent with experimental data.

Nevertheless, in the case of a biomolecular reaction, such as acetic acid–ethanol esterification, two surface kinetic mechanisms are feasible, depending on the number of catalytic sites involved in the limiting step.

The rate equation for a differential reactions with a single-site mechanism is

$$r = \frac{kp_1p_2}{1 + K_1p_1 + K_2p_2} \tag{7}$$

If the adsorption constants were high enough

$$K_1p_1 + K_2p_2 \gg 1 \tag{8}$$

eq 7 would become

$$r = k''(w_2/w_1)p_1 \tag{9}$$

where k'' is a function of the reactants ratio

$$k'' = \frac{k_1\bar{c}K_1(w_2/w_1)}{K_1 + K_2(w_2/w_1)} \tag{10}$$

This equation can be arranged to give

$$\frac{1}{k''} = \frac{K_2}{k_1\bar{c}K_1} + \frac{1}{k_1\bar{c}}\frac{1}{w_2/w_1} \tag{11}$$

showing a linear relationship between the reciprocal of the reactants ratio and the reciprocal of k'' (Figure 6).

The rate equation for a differential reaction with a dual-site mechanism is

$$r = \frac{kp_1p_2}{(1 + K_1p_1 + K_2p_2)^2} \tag{12}$$

If the hypothesis 8 were considered, the reaction rate would not be a function of p_1 but only of the reactants ratio.

If the opposite hypothesis ($K_1p_1 + K_2p_2 \ll 1$) were considered, both mechanisms would lead to a second-order potential model, which is nonconsistent with the kinetic data.

Table III. *F*-Test for Single-Site and Dual-Site Models Discrimination

model	error variance	residual variance	*F* (exptl)	*F* (calcd) (0.95)	*F* (calcd) (0.90)
single-site	0.00224	0.00399	1.78	3.3881	2.5612
dual-site	0.00224	0.00675	3.02	3.3881	2.5612

Table IV. Comparison between Global Kinetic Constant Values Obtained from a Simple Phenomenological Model (Equation 1) or from a Single-Site Model (Equation 10)

$(w_2/w_1)_m$	k', (mol·equiv^{-1}·h^{-1}·mmHg^{-1})	k'', (mol·equiv^{-1}·h^{-1}·mmHg^{-1})
0.42	0.47	0.56
0.61	0.62	0.74
1.01	0.80	1.04

Table V. Discrepancy between k' and k'' Values and Its Correspondence to the Goodness of $K_1p_1 + K_2p_2 \gg 1$ Hypothesis

$(w_2/w_1)_m$	$[(k'' - k')/k']100$	$[1/(K_1p_1 + K_2p_2)]100$
0.42	18	22
0.61	29	27
1.01	19	20

Nevertheless, if neither hypothesis 8 nor the opposite one were correct, discrimination would not be so clear. Therefore, both surface models (eq 7 and 12) were subjected to a Gauss–Seidel method fitting. Results are given in Table II.

An F-test indicates a better fitting of eq 7 than eq 12 (see Table III). Nonetheless, the statistical treatment is not fully conclusive.

From the estimated parameters of the single-site model (eq 7 and Table II), by the mentioned nonlinear fitting, k'' values were calculated by means of expression 10. These calculated values and the respective first-order rate constant k' values (eq 1 and Table I) are compared in Table IV. Though there is good agreement, it is significant that the relative small discrepancies are consistent with the assumed hypothesis that $K_1p_1 + K_2p_2 \gg 1$, as shown in Table V. This is not a new argument to favor the single-site model but a proof of the mathematical consistency of the parameters estimation.

The single-site mechanism model (eq 7), with the estimated parameters (Table II), is depicted in Figure 7. The three-dimensional surface has been projected in the r–p_1 Cartesian plane. Every curve represents a specific experimental reactants ratio. These ratio values are average ones, since this ratio varies a little through the reactor as mentioned above.

Finally, it must be pointed out that L–H–H–W models, though used by other authors in this research field, were not thought to explain the resins catalytic performance. The catalyst model in the L–H–H–W hypothesis framework does not suit the complex reality of the ion-exchange resins. Furthermore, some structural aspects of these resins are uncertain, especially in dynamic conditions.

Conclusions

Working at a constant reactants ratio and within the experimental conditions described in this work, it can be found that a first-order rate equation describes the process kinetics.

This phenomenological behavior can be liable to a L–H–H–W model, where the surface reaction is the process rate-controlling step. A single-site mechanism seems to be plausible.

The first-order rate constant follows the Arrhenius law, 4000 cal/mol being the apparent activation energy.

This low value can be explained taking into account that this first-order rate constant is a pseudokinetic constant

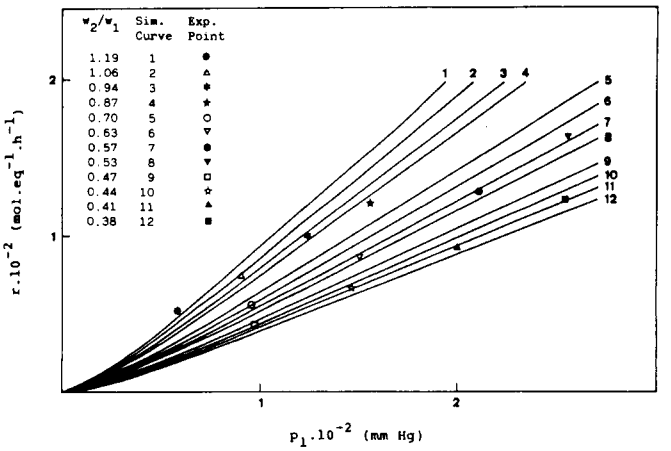

Figure 7. Reaction rate variation vs. ethanol partial pressure. Comparison between the predicted curves for the single-site mechanism and the experimental points.

which, according to the L–H–H–W models, includes the surface rate kinetic constant, the sites concentration, and the adsorption equilibrium constants.

Acknowledgment

We are grateful to the Departament d'Ensenyament de la Generalitat de Catalunya for funds received to carry out this research and to CAICYT (657/83) for computer time available to do part of the work.

Nomenclature

$\bar{c}$ = active sites concentration, mol·equiv^{-1}
F = variances ratio distribution
f = adimensional factor which relates the pressure in any reactor point with the entrance pressure and the conversion
K_i = adsorption equilibrium constant for component i, mmHg^{-1}
k = global kinetic constant, mol·equiv^{-1}·h^{-1}·mmHg^{-2}
k' = global kinetic constant, mol·equiv^{-1}·h^{-1}·mmHg^{-1}
k'' = global kinetic constant, mol·equiv^{-1}·h^{-1}·mmHg^{-1}
k_1 = kinetic constant for direct reaction, h^{-1}
L–H–H–W = Langmuir–Hinshelwood–Hougen–Watson model
P = total pressure, mmHg
p_i = partial pressure for component i, mmHg
Q = acid equivalents of catalyst, equiv
R = gas constant, cal·mol^{-1}·K^{-1}
r = reaction rate, mol·equiv^{-1}·h^{-1}
T = temperature, K
w_i = molar flow rate of component i, mol·h^{-1}
X_i = fractional conversion referred to component i
x_i = molar fraction of component i
Y' = parameter used in the integral treatment according to eq 5, mmHg^{-1}

Subscripts

E = inlet or entrance to the reactor
i = component i
1 = ethyl alcohol
2 = acetic acid

Registry No. Acetic acid, 64-19-7; Amberlyst 15, 9037-24-5.

Literature Cited

Amundson, N. R.; Stusiak, M. **1959**, *P B Rept.* 136776.
Andrianova, T. I. *Katal. Reakts. Zhidk. Faze, Tr. Vses. Konf.* **1962**, 428–432; *Chem. Abstr.* **1980**, *60*, 13108g.
Andrianova, T. I. *Kinet. Katal.* **1964**, *5*, 927–931.

Andrianova, T. I.; Bruns, B. P. *Kinet. Katal.* **1960**, *1*, 440-446.
Ballesteros, A.; García de la Banda, J. F.; Hermana, E. *Anal. Fís. Quím.* **1967**, *63*, 179-190.
Buckley, R. A.; Altpeter, R. J. *Chem. Eng. Prog.* **1951**, *47*, 243-250.
Chashchin, A. M. *Sb. Tr. Tsentr. Nauchn.-Issled. Proektn. Inst. Lesokhim. Prom. Sti.* **1963**, *15*, 30-42; *Chem. Abstr.* **1982**, *62*, 8959h).
Costa, J.; Cervera, S.; Giménez, J. *Afinidad* **1984**, *41*, 323-327.
Hawes, R. W.; Kabel, R. L. *AIChE J.* **1968**, *14*, 606-611.
Herrman, A. J. Ph.D. Dissertation Series, Publication 12.131, University Microfilms, Ann Arbor, MI, 1955.
Hoerig, H. F.; Hanson, D.; Kowalke, O. L. *Ind. Eng. Chem.* **1943**, *35*, 575-580.
Polyanskii, N. G.; Sapozhnikov, V. K. *Usp. Khim.* **1977**, *46*, 445-476.
Potter, A. E., Jr.; Bender, P.; Ritter, H. L. *J. Phys. Chem.* **1955**, *59*, 250-254.
Santacesaria, E.; Gelosa, D.; Danise, P.; Carra, S. *J. Catal.* **1983**, *80*, 427-436.
Sinisterra, J. V.; Morey, J.; Marinas, J. M. *Afinidad* **1979**, *36*, 305-309.
Venkateswarlu, C.; Satyanarayana, M.; Rao, M. N. *Ind. Eng. Chem.* **1958**, *50*, 973-978.

Received for review February 20, 1986
Revised manuscript received April 29, 1986
Accepted September 9, 1986

Enhanced Coal Liquefaction with Steam Pretreatment

Paul R. Bienkowski, Ramani Narayan, Robert A. Greenkorn, and Kwang-Chu Chao*
School of Chemical Engineering, Purdue University, West Lafayette, Indiana 47907

A two-step process for the liquefaction of coal, in a semiflow microreactor, was investigated. The process consisted of pretreating coal with low-temperature steam, followed by treatment with supercritical steam. The maximum observed conversion of a Wyodak subbituminous coal, using this two-step process, was 40 wt % on a moisture- and ash-free basis (MAF). The 240 °C pretreatment step resulted in a 32% increase over the conversion observed with just a 400 °C treatment. The coal liquid obtained has a number average molecular weight of 325 and a mass average molecular weight of 373, with a narrow molecular weight distribution. The hydrogen and oxygen content of the extract is increased; a significant amount of the oxygen is present as dihydroxy aromatics. A highly condensed residue of lower hydrogen and oxygen content is obtained which can be of value as a solid fuel.

Recent investigations have led to the observation (Atherton and Kulik, 1982) that in its native unweathered state coal is a reactive material, with extensive hydrogen bonds connecting the polynuclear aromatic clusters to form a semipermanent macromolecular structure. The structure is particularly fragile in subbituminous coals and may be subject to rupture with mild treatment to dissociate the hydrogen bonds. Graff and Brandes (Anon, 1985) found that carbon conversion to liquids in pyrolysis at 940 °C was raised from 23% to over 50% if the coal was exposed to steam for times of less than 30 min at temperatures between about 320 and 360 °C. Both pretretment and pyrolysis were conducted in 50 atm of steam. This result suggests that coal is partially depolymerized by the steam pretreatment, perhaps by the removal of oxygen linkages. If this is indeed the case, improved yields and/or lighter liquids should result if the pretreated coal is liquefied instead of pyrolyzed.

Experimental Section

Wyodak coal was pretreated and treated with steam in a semiflow microreactor at controlled conditions to exclude oxygen. The apparatus is depicted in Figure 1. The main components are a Milton Roy metering pump (29-290 cm^3/h) which provides a continuous and constant flow of distilled deoxygenated water to the reactor, a Tecam fluidized sand bath (Model SBS-4) controlled with a Leeds and Northrup controller (Electromax III), a Helicoid pressure gauge (0-3000 psig), an autoclave micrometering valve, and a microreactor equipped with a sheathed thermocouple (see Figure 2).

The feed material was an unweathered subbituminous Wyodak coal provided by EPRI in a water slurry kept in a sealed air-tight barrel (No. 4171). Table I shows the elemental analysis of samples taken from this barrel. Samples A and B were taken from the top and middle of the barrel and were suction dried for use. These were the main feed material. About a 50-g sample of this material was removed from the barrel and vacuum dried; a sample of this material is reported as sample C. A few reactions were carried out with this material.

Table I. Analysis of Wyodak Coal[a]

	sample		
	A, wet	B, wet	C, vacuum dried
C	59.51	59.72	58.17
H	4.79	4.13	4.35
O	17.90	22.44	18.94
N	0.79	0.76	0.63
Cl			
S	2.97	2.55	3.07
ash	13.59	13.47	16.46
total	99.55	103.07	101.62
btu/lb	10614		10141

[a] Analysis of samples was performed by Huffman Laboratory.

The suction-dried coal was prepared in a Büchner filter, by applying suction to it for about 1 h. The top portion of the material was removed from the filter and thoroughly mixed to ensure a homogeneous sample for reaction. The moisture content of this material (≈30 wt %) was determined by weighing a sample before and after further drying in a vacuum oven at 45 °C for 6 h. Duplicate samples were used for moisture determinations.

Suction-dried Wyodak coal is pastelike, and is messy to handle. A free-flowing coal powder was obtained for reaction experiments by drying the coal in vacuum under mild heating. The vacuum-dried coal was prepared by suction drying in a Büchner funnel over nitrogen; the material was then transferred in a jar filled with nitrogen, to a vacuum oven and dried for 72 h at 45 °C. The experimental reaction procedure for vacuum-dried coal was similar to suction dried coal except that the separate

0888-5885/87/2626-0202$01.50/0